ISSN 2616-5767 Vol.9, Issue 3: 77-87, DOI: 10.25236/AJETS.2026.090311

Design of an ultrasonic monitoring system for wind turbine blade root bolts based on embedded technology

Lipeng Peng[1,a], Shuyi Yang[1,b], Yaowei Song[1,c]

[1]School of Mechanical and Electrical Engineering, Hunan University of Science and Technology, Xiangtan, China
[a]710167591@qq.com, [b]ysy822@126.com, [c]2605673256@qq.com

Abstract: *As one of the important connecting components of wind turbines, the damage status of blade root bolts is closely related to the safety of wind turbines. However, traditional operation and maintenance methods cannot detect damaged bolts in a timely and accurate manner. Therefore, this paper designs an embedded-based ultrasonic monitoring system for blade root bolts of wind turbines. The monitoring system, with embedded chips and FPGA chips as its core, combines high-performance ultrasonic chips and ADC chips to achieve ultrasonic detection of blade root bolts. Through algorithms, damage characteristics in the signal are extracted and analyzed to automatically identify the current working state of the blade root bolt and determine whether there is damage. Experimental results show that the monitoring system can effectively acquire the slight time difference caused by the deformation of the bolt under stress, and calculate an ultrasonic stress coefficient of 0.585.*

Keywords: *blade root bolt; ultrasonic testing; embedded technology; FPGA technology*

1. Introduction

As one of the crucial connecting components on wind turbines, the blade root bolt plays a significant role in connecting and securing the blades to the hub. Its connection status is closely linked to the safe and stable operation of the wind turbine. However, during operation, the blade root bolt often bears the combined effects of multiple complex loads such as aerodynamic loads, gravitational loads, and inertial loads[1,2], gradually accumulating fatigue damage. This makes the blade root bolt highly susceptible to loosening, cracking, or fracture, which in turn may lead to accidents such as blade detachment and wind turbine damage, posing a threat to the safety of the wind turbine. Traditional operation and maintenance methods rely on manual regular inspections and irregular spot checks to eliminate damaged bolts; however, they rely heavily on human experience, which may lead to missed or incorrect inspections. Additionally, the blade root bolt is installed on a wind wheel hundreds of meters high, making inspection difficult. Therefore, there is an urgent need for a detection device to replace manual inspection. This device uses hardware circuits composed of chips and sensors to detect the blade root bolt, and then utilizes software algorithms to process and analyze the detection data, thereby identifying the current connection status of the blade root bolt.

Ultrasonic detection technology, as a crucial method in industrial non-destructive testing, has seen its hardware platform evolve alongside the enhancement of electronic device integration and processing capabilities. Early systems were predominantly constructed using discrete components and analog circuits, resulting in complex structures and rigid functionality. With the widespread adoption of microcontrollers (MCU) and digital signal processors (DSP), digital ultrasonic detection systems have progressively achieved programmability in signal processing. In recent years, embedded technology and FPGA technology, leveraging their parallel processing architecture and hardware reconfigurability, have demonstrated significant advantages in ultrasonic emission control, high-speed data acquisition, and real-time signal processing, becoming the core platform for constructing high-performance ultrasonic detection systems. For instance, Liu Lin et al.[3] designed a portable ultrasonic thickness gauge based on ARM and FPGA chips; Pang Song et al.[4] developed a bolt stress monitoring system based on ZYNQ.

The development of ultrasonic detection signal processing technology has always revolved around two core objectives: noise suppression and precise extraction of feature parameters. Early methods mainly relied on time-domain thresholding to directly interpret echo positions, but were prone to

ISSN 2616-5767 Vol.9, Issue 3: 77-87, DOI: 10.25236/AJETS.2026.090311

misinterpretation due to noise interference[5]. With the introduction of digital signal processing technology, denoising methods such as frequency-domain filtering and wavelet transform have been widely applied in the preprocessing of ultrasonic signals, effectively improving the signal-to-noise ratio[6,7]. In terms of time-of-flight measurement, for large-scale defects such as cracks and fractures, thresholding methods are commonly used due to their simplicity and efficiency; whereas for subtle time shifts caused by minor deformations such as bolt loosening, cross-correlation analysis algorithms have become the mainstream solution due to their high-precision advantage in estimating the time delay of weak signals. Xu Xiao et al.[8] utilized the cross-correlation algorithm to obtain the transit time difference to characterize the stress state of bolts in the study of high-strength bolt axial force detection; Lu Yan et al.[9] also employed the cross-correlation algorithm to acquire the transit times of longitudinal and shear waves. This paper will design an ultrasonic monitoring system for fan blade root bolts based on embedded technology, combining FPGA technology to achieve high-precision ultrasonic signal transmission and reception, signal acquisition, etc., and utilize signal processing technology to process and analyze ultrasonic signals, thereby obtaining damage state information of the blade root bolts.

2. Ultrasonic detection principle

The core principle of ultrasonic testing technology[10] is as follows: high-frequency sound waves encounter physical phenomena such as reflection and refraction when propagating inside materials upon encountering interfaces (such as defects and bottom surfaces). By capturing and analyzing these echoes, invisible information inside the material can be detected. Longitudinal or transverse waves are commonly used to test the tested object[11,12], and in some scenarios, other types of sound waves such as surface waves and guided waves are also employed for testing[13,14]. Ultrasonic testing employs various methods such as pulse echo method, penetration method, and time-of-flight diffraction method to inspect major components or important connectors of wind turbines[15-17], such as tower tubes, blades, and bolts.

For the detection of loosening in blade root bolts, ultrasonic testing technology is primarily used to measure the stress on the blade root bolts, thereby obtaining information about the loosening state. When the blade root bolt is under stress, it can be regarded as a mechanical spring, and the changes caused by the pre-tightening force can be simplified as the deformation of a mechanical spring under tensile force[18]. The amount of deformation satisfies Hooke's law. When the blade root bolt is under stress, ultrasonic testing can reveal that the flight time of the ultrasonic wave is slightly extended compared to when it is not under stress. According to the calculation method in "VDI_2230 System Calculation for High-Strength Bolt Connections"[18], the amount of deformation ΔL is

$$\Delta L = \frac{FL_0}{EA} \tag{1}$$

Where F is the preload on the root bolt, E is Young's modulus, A is the stress area, and L_0 is the length of the root bolt when unloaded. Then, the length L_σ of the root bolt under this condition is given by

$$L_\sigma = L_0 + \Delta L \tag{2}$$

Meanwhile, the preload on the root bolt also affects the propagation velocity of ultrasound within the bolt. Denoting the ultrasonic velocity in the bolt under load as v_σ, the ultrasonic velocity v_σ under this condition is given by

$$v_\sigma = v_0(1 + K_L\sigma) \tag{3}$$

Where K_L is the acoustoelastic coefficient and σ is the stress. Therefore, when the root bolt is subjected to a preload F, the round-trip time t_σ of the ultrasonic wave propagating back and forth within the root bolt is given by

$$t_\sigma = \frac{2L_\sigma}{v_\sigma} \tag{4}$$

And when the root bolt is unloaded, the round-trip time t_0 of the ultrasonic wave propagating back and forth within the bolt is given by

$$t_0 = \frac{2L_0}{v_0} \tag{5}$$

By combining and rearranging equations (1) to (5), we obtain

$$t_\sigma = \frac{\left(1+\frac{F}{EA}\right)t_0}{1+K_L\sigma} \tag{6}$$

ISSN 2616-5767 Vol.9, Issue 3: 77-87, DOI: 10.25236/AJETS.2026.090311

Generally, the acoustoelastic coefficient K_L of steel is very small, so $K_L\sigma \ll 1$. Therefore, equation (6) can be simplified as

$$t_\sigma = t_0 + \frac{t_0}{EA}F \tag{7}$$

Let $K=EA/t_0$, then the following relationship can be obtained

$$F = K(t_\sigma - t_0) \tag{8}$$

From this, a relationship between preload force and time difference can be derived, where K is the ultrasonic stress coefficient that needs to be calibrated. The derivation of the above formula is based on ideal conditions, ignoring the influence of factors such as temperature and coupling state. In practical situations, ultrasonic stress detection is affected by various factors[19], making the relationship between preload force and time difference not a direct proportional function passing through the origin. Therefore, a constant term needs to be added to formula (8) for correction, as shown in formula (9), where b is the constant term used for correction.

$$F = K(t_\sigma - t_0) + b \tag{9}$$

Through this relationship, ultrasonic detection technology can be utilized to measure the force currently exerted on the blade root bolt and obtain information about the magnitude of the force, thereby indirectly determining whether the blade root bolt is loose or damaged.

When cracks or fracture damage exist in the blade root bolt, ultrasonic waves will reflect off the crack or fracture surface. The reflected sound waves will produce a small pulse signal on the signal waveform diagram, or a pulse signal similar to the bottom echo, as shown in Figure 1. The crack echo will appear between the transmitted signal and the bottom echo, and its occurrence time and signal amplitude are usually related to the location and size of the crack. The closer the crack is to the ultrasonic probe, the earlier the crack echo appears; the larger the signal amplitude of the crack echo, the larger the crack in the blade root bolt, reflecting more ultrasonic waves. Therefore, by analyzing the time and amplitude of the crack echo, the location and size of the crack in the blade root bolt can be calculated. The fracture echo is only related to time. Ultrasonic waves will be totally reflected at the fracture surface, and its signal amplitude is consistent with the bottom echo. Therefore, when a pulse signal with an amplitude similar to the bottom echo but occurring earlier than the bottom echo is detected, it indicates that the blade root bolt has fractured.

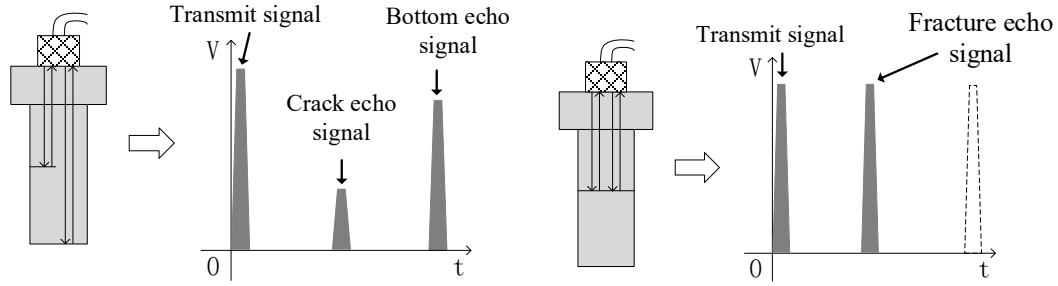

(a) When there are cracks in the bolt *(b) When the bolt breaks*

Figure 1 Ultrasonic signal when the bolt has cracks or fractures

3. System hardware circuit design

3.1 System overall and main control circuit design

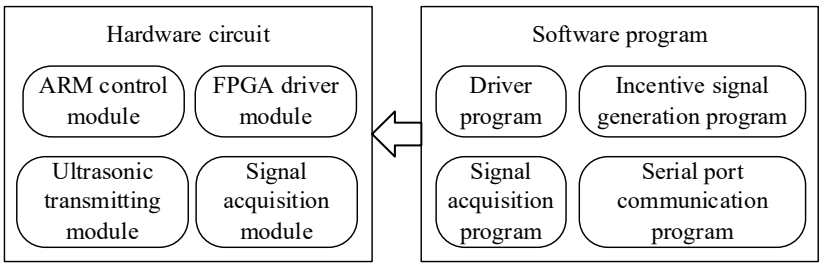

Figure 2 Overall system framework

ISSN 2616-5767 Vol.9, Issue 3: 77-87, DOI: 10.25236/AJETS.2026.090311

As shown in Figure 2, this is the overall framework diagram of the ultrasonic monitoring system for wind turbine root bolts (hereinafter referred to as the monitoring system). The monitoring system consists of two parts: hardware circuitry and software programs. The hardware circuitry provides the foundation for system functions, enabling ultrasonic testing, signal acquisition, and other capabilities. The software programs drive the hardware circuitry, accomplishing functions such as excitation signal generation, ADC data acquisition, as well as signal processing and analysis.

The hardware circuit design primarily consists of two parts: the ARM control module and the FPGA drive module. The ARM control module, centered around an ARM architecture chip, is primarily responsible for overall system control, data storage, and processing. The main control chip is an embedded chip from the Cortex-A7 series, with a maximum frequency of up to 800MHz. The FPGA drive module, centered around an FPGA chip, is primarily responsible for controlling components such as ultrasonic chips and ADC chips, providing the hardware foundation for ultrasonic detection functions. Figure 3 depicts the hardware circuit framework.

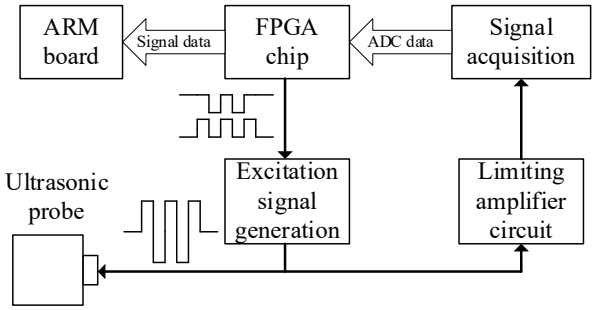

Figure 3 Hardware Circuit Framework Diagram

The main control circuit comprises two parts: the ARM main control and the FPGA minimal system. The ARM main control is an embedded development board that implements system control, signal processing, and display functions based on the Linux system. The FPGA minimal system, centered around the XC6SLX9 and paired with a Flash chip and an active crystal oscillator, is responsible for clock frequency division, ultrasonic drive signal generation, ADC data reception, and other functions, and communicates with the ARM through a serial port. Figure 4 depicts the circuit framework of the FPGA minimal system.

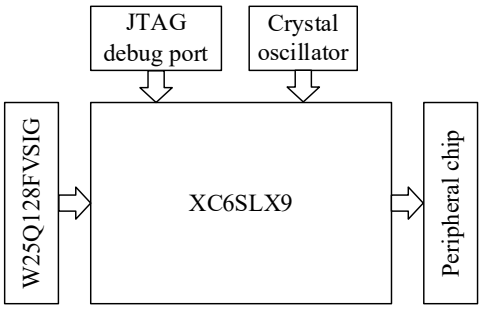

Figure 4 FPGA minimum system framework diagram

3.2 Ultrasonic signal transmitting circuit

The monitoring system uses a piezoelectric ultrasonic probe, which requires a high-voltage excitation signal to cause the piezoelectric crystal to vibrate and generate ultrasound. The ultrasonic signal transmission circuit employs two chips, MD1213 and TC6320, to generate this high-voltage excitation signal, thereby driving the ultrasonic probe to transmit ultrasonic waves.

As shown in Figure 5, this is the schematic diagram of the ultrasonic signal transmission circuit. The input pins INA and INB of the MD1213 receive 3.3 V logic signals (provided by the FPGA chip). When the power supply pins VH, VL, VSS, and VDD are supplied with ±5 V, a driving signal with a peak-to-peak voltage of 10 V can be detected at the output pins OUTA and OUTB. The frequency and waveform of the driving signal remain consistent with those of the 3.3 V logic signal.

ISSN 2616-5767 Vol.9, Issue 3: 77-87, DOI: 10.25236/AJETS.2026.090311

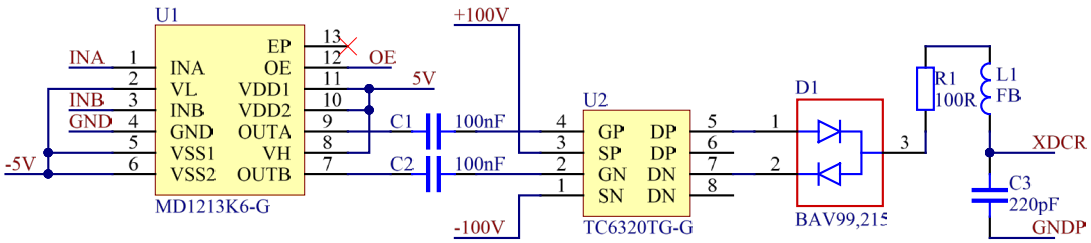

Figure 5 Schematic diagram of ultrasonic generation circuit

As shown in Figure 6, the signal waveforms obtained when the output pins OUTA and OUTB are measured with an oscilloscope are presented. The magenta line represents the signal at OUTA, and the yellow line represents the signal at OUTB. Both signals are square waves with a frequency of 2.5 MHz and a peak-to-peak voltage of 10 V.

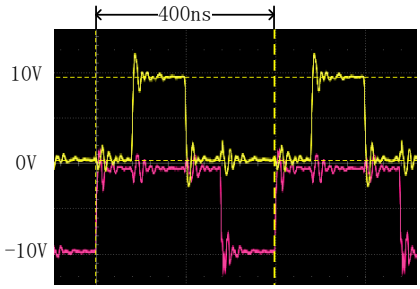

Figure 6 Waveform diagram of output pin

Capacitors C1 and C2 are bootstrap capacitors. By utilizing the characteristic that the voltage across a capacitor cannot change instantaneously, they bootstrap the 10 V driving signal to near the source voltage of each MOS transistor, thereby preventing the gate-source voltage Vgs from exceeding the maximum rating and damaging the MOS transistors. Under the control of the driving signal, the TC6320 alternately turns on the P-channel and N-channel transistors to output the source voltage (±100 V), thereby generating a high-voltage excitation signal at a specific frequency, which is then output to the ultrasonic probe. When performing ultrasonic testing on root bolts, the ultrasonic probe does not need to emit ultrasonic waves continuously; typically, only a few cycles are required. Therefore, the high-voltage excitation signal is usually a pulse signal with a duration of several microseconds. As shown in Figure 7, this is the high-voltage excitation signal during testing. The peak-to-peak voltage of the signal is 185 V, the signal frequency is 2.5 MHz (determined by the 3.3 V logic signal), and the pulse width is 10 μs. It can be observed from the figure that the signal is followed by a trailing ring, which is caused by the fact that the voltage across capacitor C3 cannot change abruptly. This trailing ring has little effect on the excitation signal.

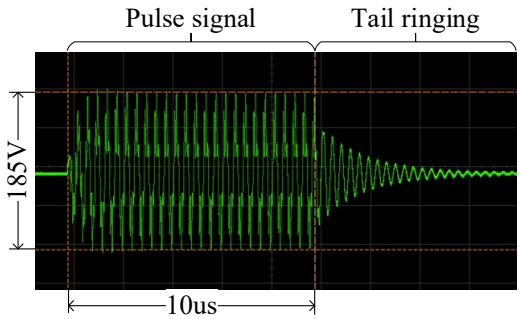

Figure 7 10us excitation signal

3.3 Limiting amplification and signal acquisition circuit

Since ultrasonic echo signals typically have an amplitude of only a few millivolts, and the high-voltage excitation signal that drives the probe can also couple into the acquisition circuit, it is necessary to amplify the ultrasonic echo signal and limit the amplitude of the high-voltage excitation signal. As shown in Figure 8, this is the schematic diagram of the limiting amplifier circuit. Before the ultrasonic

ISSN 2616-5767 Vol.9, Issue 3: 77-87, DOI: 10.25236/AJETS.2026.090311

echo signal enters the amplification circuit, it first passes through limiting diodes that restrict the signal amplitude to within ±1 V, preventing high voltages from damaging the chip. The signal is then amplified by the AD8331 and converted into a differential output. The AD8331 is a high-performance variable gain amplifier capable of providing controllable gain amplification from 0 to 55.5 dB. It can also convert a single-ended input signal into a differential output (output pins VOH and VOL), thereby improving the signal's immunity to interference.

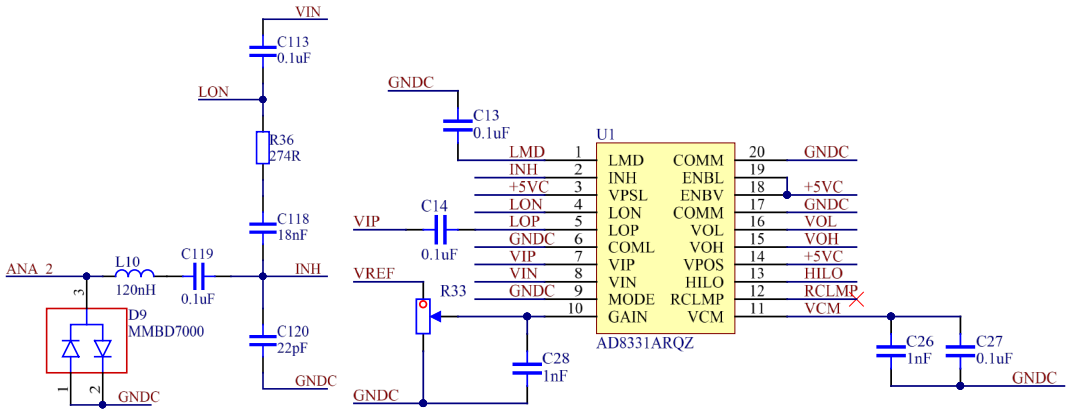

(a) Limiting circuit *(b) amplifier circuit*

Figure 8 Schematic diagram of limiting amplifier circuit

After passing through the limiting amplifier circuit, the ultrasonic echo signal is output as a differential signal. Before entering the signal acquisition circuit, it must also pass through a low-pass filter circuit, as shown in Figure 9. This low-pass filter circuit serves as an anti-aliasing low-pass filter at the ADC front end. Its primary function is to limit the bandwidth of the input signal, filter out high-frequency noise, and prevent spectral aliasing during the analog-to-digital conversion process.

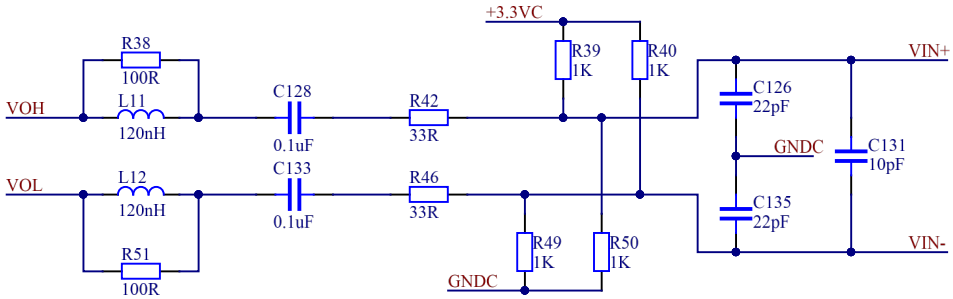

Figure 9 Low-pass filter circuit

The signal acquisition circuit is an analog-to-digital conversion circuit centered around the AD9215. The schematic diagram of the circuit is shown in Figure 10. The AD9215 is a 10-bit, high sampling rate, low-power analog-to-digital converter. It supports a maximum sampling rate of up to 105 MHz, with an input range of ±1 V and a resolution of approximately 0.001 V, providing high detection accuracy.

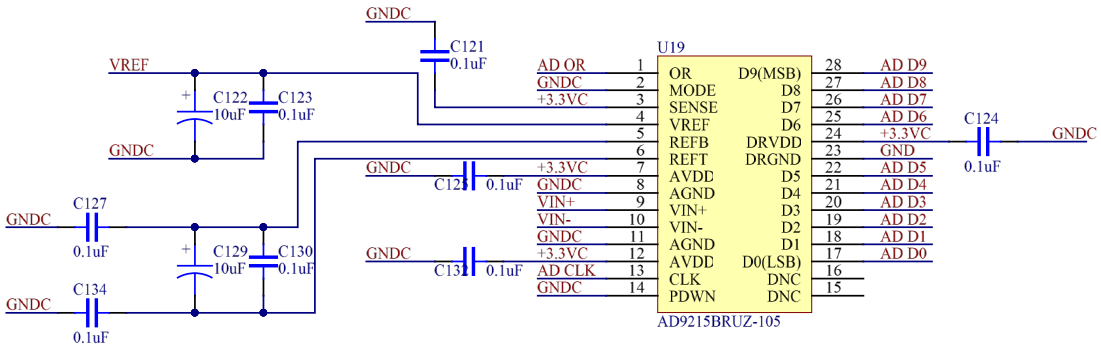

Figure 10 Schematic diagram of signal acquisition circuit

ISSN 2616-5767 Vol.9, Issue 3: 77-87, DOI: 10.25236/AJETS.2026.090311

The differential signal output from the limiting amplifier circuit is fed into the input pins VIN+ and VIN- of the AD9215. After conversion, the level signals are directly output from pins D0 to D9. Therefore, the FPGA chip only needs to read the level values on these pins and store them to complete a single data acquisition. However, the AD9215 has an output delay time of 2.5 ns to 6.5 ns. Consequently, a delay of several nanoseconds is required after the rising edge to allow the data to stabilize before reading.

4. System software programming design

4.1 Hardware circuit driver program

The hardware circuit driver is developed using Verilog language and is primarily implemented on the FPGA control module to achieve functions such as ultrasonic signal generation, reception, and storage. As shown in Figure 11, this is the hardware driver flowchart. After the embedded system issues a start command, the FPGA chip generates a 2.5 MHz square wave signal and outputs it to the ultrasonic signal transmission circuit. Based on the input signal, the ultrasonic signal transmission circuit generates a 2.5 MHz excitation signal of approximately ±95 V and outputs it to the ultrasonic probe, causing it to emit ultrasonic waves. The system then waits for the ultrasonic probe to receive the echo signal and output it to the limiting amplifier circuit and the signal acquisition circuit, where the echo signal is limited, amplified, filtered, and then converted from analog to digital to obtain signal data. The acquired data is temporarily stored in the FIFO core of the FPGA and subsequently sent to the embedded system via a serial port for processing and analysis.

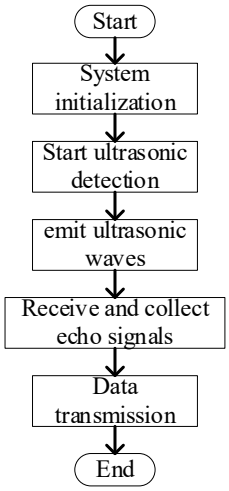

Figure 11 Hardware Driver Flowchart

4.2 Signal processing program

The raw ultrasonic signal acquired through the circuit contains a significant amount of interference and cannot be directly used for signal analysis. Therefore, it is necessary to perform essential signal preprocessing on the raw ultrasonic signal to remove the interfering components and improve the signal-to-noise ratio. In this paper, bandpass filtering and wavelet transform algorithms are employed for signal preprocessing to filter and denoise the raw ultrasonic signal, eliminating interference[20,21], and to extract the ultrasonic signal at a frequency of 2.5 MHz used for system detection, which will be subsequently utilized for root bolt condition analysis. Equation (10) defines the continuous wavelet transform as follows

$$W(a,b) = \frac{1}{\sqrt{|a|}} \int_{-\infty}^{+\infty} x(t)\psi^* \left(\frac{t-a}{a}\right) \mathrm{d}t \tag{10}$$

As shown in Figure 12, this is the site diagram of the calibration experiment for the ultrasonic stress coefficient. The fatigue testing machine is an operational device within the PWS-100 electro-hydraulic servo high-temperature fatigue testing system manufactured by Zhongji Testing Equipment Co., Ltd. Through the system's control interface, users can set the tensile force applied by the fatigue testing machine to simulate the preload experienced by the wind turbine root bolt during operation. The actual load range that the fatigue testing machine can apply is 0 to 40 kN; therefore, the bolt deformation is

ISSN 2616-5767 Vol.9, Issue 3: 77-87, DOI: 10.25236/AJETS.2026.090311

only tested within this range. The upper and lower fixtures are used to secure the test bolt and transmit the load. The test bolt is an undamaged grade 4.8 M20 bolt, and the bolt head has been surface-treated to make it flat and smooth. Before installing the ultrasonic probe, a dedicated industrial ultrasonic couplant is applied to the bolt head surface to facilitate better transmission of ultrasonic waves into the test bolt.

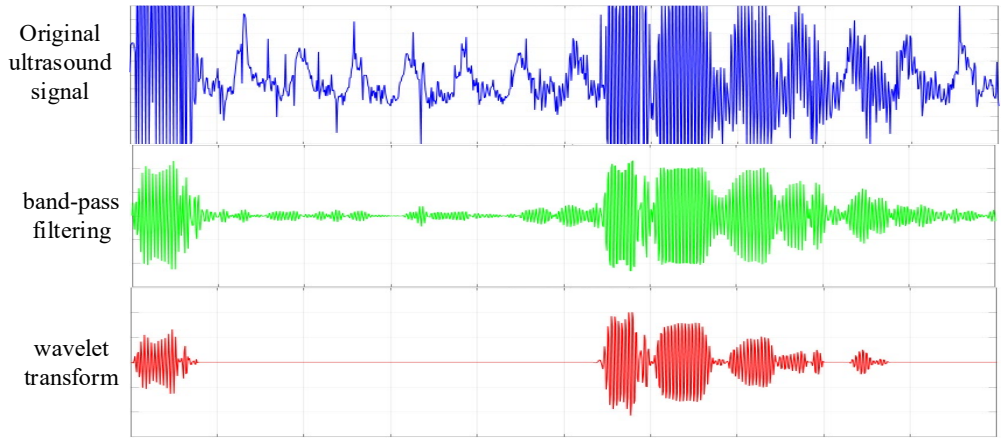

Figure 12 Waveform diagrams of the original ultrasound signal, the signal after band-pass filtering, and the signal after wavelet transformation

In signal analysis, the time-of-flight of the ultrasonic wave is calculated using the threshold method and the cross-correlation analysis algorithm to assess damage such as loosening or cracking of the root bolt[22,23]. The threshold method determines the arrival time of the echo signal by setting a voltage amplitude threshold and identifying the first time the echo signal exceeds this threshold, enabling rapid extraction and judgment of signal features. However, this method is highly sensitive to noise; the lower the signal-to-noise ratio, the poorer the detection accuracy. Therefore, it is typically used for rapid screening. In the cross-correlation algorithm, the reference signal x[n] is defined as the envelope signal of the root bolt under an unloaded condition, and the measurement signal y[n] is defined as the envelope signal of the root bolt under a loaded condition. The cross-correlation function is then defined as follows

$$R_{xy}[k] = \sum_{n=-\infty}^{\infty} x\,[n] \cdot y[n+k] \tag{11}$$

To effectively extract the nanosecond-level time shift in the ultrasonic signal, the normalized cross-correlation function is commonly used to eliminate the influence of signal amplitude, as shown in Equation (12)

$$\rho_{xy}[k] = \frac{\sum_{n=0}^{N-1}(x[n]-\bar{x})(y[n+k]-\bar{y})}{\sqrt{\sum_{n=0}^{N-1}(x[n]-\bar{x})^2 \sum_{n=0}^{N-1}(y[n]-\bar{y})^2}} \tag{12}$$

For ultrasonic signal analysis of root bolts, the threshold method is first used to rapidly screen for crack echoes and fracture echoes, in order to determine whether the root bolt has cracked or already fractured. Then, the cross-correlation analysis algorithm is employed to accurately calculate the current deformation of the root bolt, thereby obtaining the minute time difference. Based on the functional relationship between preload and time difference, it can be determined whether the root bolt has become loose.

5. System testing experiment

Based on the above hardware circuitry and software programs, an ultrasonic monitoring system for wind turbine root bolts has been developed. To enable the system to detect loosening, it is first necessary to calibrate the ultrasonic stress coefficient K and establish the functional relationship between the bolt load and the ultrasonic time-of-flight, as shown in Equation (9). Figure 13 presents the physical diagram of the FPGA circuit board.

ISSN 2616-5767 Vol.9, Issue 3: 77-87, DOI: 10.25236/AJETS.2026.090311

Figure 13 Physical image of FPGA circuit board

As shown in Figure 14, this is the site diagram of the calibration experiment for the ultrasonic stress coefficient. The fatigue testing machine is an operational device within the PWS-100 electro-hydraulic servo high-temperature fatigue testing system manufactured by Zhongji Testing Equipment Co., Ltd. Through the system's control interface, users can set the tensile force applied by the fatigue testing machine to simulate the preload experienced by the wind turbine root bolt during operation. The actual load range that the fatigue testing machine can apply is 0 to 40 kN; therefore, the bolt deformation is only tested within this range. The upper and lower fixtures are used to secure the test bolt and transmit the load. The test bolt is an undamaged grade 4.8 M20 bolt, and the bolt head has been surface-treated to make it flat and smooth. Before installing the ultrasonic probe, a dedicated industrial ultrasonic couplant is applied to the bolt head surface to facilitate better transmission of ultrasonic waves into the test bolt.

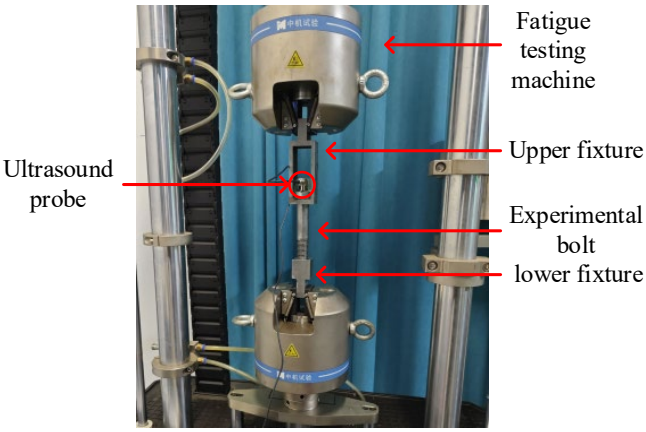

Figure 14: Site photo of calibration experiment

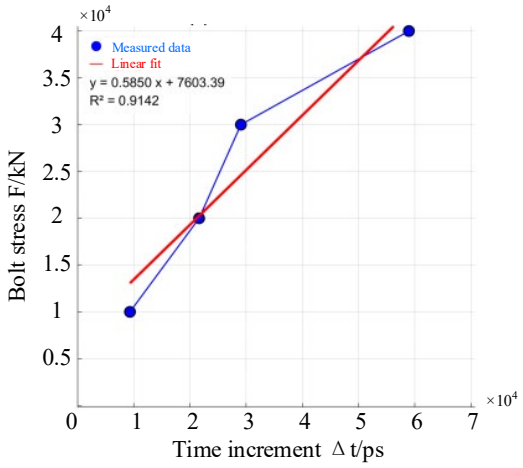

Figure 15 Bolt stress and time increment

In the calibration experiment for the ultrasonic stress coefficient, a tolerance of 10 kN is used, and the ultrasonic time-of-flight within the bolt is tested under loads ranging from 0 to 40 kN. Using the cross-correlation analysis algorithm, the ultrasonic signal under 0 kN is taken as the reference signal,

ISSN 2616-5767 Vol.9, Issue 3: 77-87, DOI: 10.25236/AJETS.2026.090311

while the ultrasonic signals under other loads are taken as the measurement signals, to calculate the time-of-flight differences under different loads. The ultrasonic time-of-flight differences from 10 kN to 40 kN are 9.3 ns, 21.6 ns, 29.1 ns, and 58.9 ns, respectively. Using MATLAB's data processing functions and fitting methods, the image of the test data and the fitted functional relationship are obtained. The experimental results are shown below. Figure 15 presents the curve of bolt load versus time increment, where the blue polyline represents the test data curve and the red straight line represents the linearly fitted curve.

Equation (13) represents the functional relationship of the fitted curve, where x is the time increment (unit: ps) and y is the bolt force (unit: N). Through correlation calculation, R2 is found to be 0.9142, indicating a high correlation in the fitted function. From the equation, the ultrasonic stress coefficient in this experiment is determined to be 0.585.

$$y = 0.585x + 7603.39 \tag{13}$$

6. Conclusion

This article designs an ultrasonic monitoring system for wind turbine blade root bolts based on embedded technology. The monitoring system, centered around an embedded chip and an FPGA chip, utilizes a high-performance ultrasonic chip and an ADC chip to achieve ultrasonic detection of blade root bolts. The main conclusions are as follows:

(1) The hardware circuit of the ultrasonic monitoring system for wind turbine blade root bolts was designed based on embedded technology and FPGA technology. The embedded development board with ARM chip as the core provides overall control, signal processing and analysis, etc. for the system, while the FPGA circuit with XC6SLX9 as the core provides ultrasonic transceiving, signal acquisition, and other functions for the system.

(2) The software program for the ultrasonic monitoring system of fan blade root bolts was designed. The hardware circuit driver program was developed using Verilog language, achieving the ultrasonic detection function of the system. The ultrasonic signals were filtered and denoised using band-pass filtering and wavelet transform algorithms, effectively improving the clarity and signal-to-noise ratio of the ultrasonic signals. The signal analysis program was designed using thresholding and cross-correlation analysis algorithms for system analysis and damage feature identification.

(3) An ultrasonic stress coefficient calibration experiment was conducted. Through this experiment, a functional relationship between bolt stress and time difference was obtained, allowing the calculation of the ultrasonic stress coefficient. The ultrasonic stress coefficient was found to be 0.585, and the correlation coefficient R2 of the fitted function between bolt stress and time difference was 0.9142, indicating a strong correlation. This result lays a foundation for further research.

Acknowledgements

The paper was funded bythe Provincial Natural Science Foundation of Hunan, China (No. 2024JJ8274).

References

[1] Li Z P. Load Characteristic Analysis of Blade Root Bolt Connection Structure in Wind Turbine [D]. Hunan University of Science and Technology, 2024.
[2] Verma A S, et al. A review of impact loads on composite wind turbine blades: Impact threats and classification[J]. Renewable and Sustainable Energy Reviews, 2023, 178: 113261.
[3] Liu L, Zhao H F. Design of Portable Ultrasonic Thickness Gauge Based on ARM [J]. Instrument Technique and Sensor, 2019, (08): 36-39.
[4] Pang S, Wang X M, Ni W B. Design of Embedded Multi-bolt Stress Monitoring System for Wind Turbine [J]. Electronic Measurement Technology, 2021, 44(04): 166-171.
[5] Cheng F L, Zhou Q X, Qiu F F, et al. Ultrasonic Axial Stress Measurement Algorithm for Bolts Based on Threshold and Cross-Correlation [J]. Nondestructive Testing, 2024, 46(09): 75-82.
[6] Pardo E, San Emeterio J L, Rodriguez M A, et al. Noise reduction in ultrasonic NDT using undecimated wavelet transforms[J]. Ultrasonics, 2006, 44: e1063-e1067.
[7] Zhou Z J, Wen Z J, Bu Y M. Application of Wavelet Denoising in Ultrasonic Echo Signal Processing

ISSN 2616-5767 Vol.9, Issue 3: 77-87, DOI: 10.25236/AJETS.2026.090311

[J]. Chinese Journal of Scientific Instrument, 2009, 30(02): 237-241.
[8] Xu X, Jiang T, Jin C, et al. Research on axial force measurement technology for high-strength bolts based on ultrasonic wave [J]. Journal of Electronic Measurement and Instrumentation, 2024, 38(12): 163-172.
[9] Lyu Y, Xie L Y, Song G R, et al. Bolt Axial Stress Measurement Method Based on Acoustoelastic Effect [J]. Journal of Beijing University of Technology, 2022, 48(09): 920-927.
[10] Ensminger D, Bond L J. Ultrasonics: fundamentals, technologies, and applications[M]. Boca Raton: CRC Press, 2024.
[11] Zhu X H, et al. Damage identification of wind turbine blades based on deep learning and ultrasonic testing[J]. Nondestructive Testing and Evaluation, 2025, 40(2): 508-533.
[12] Lyu H T, Jiao J P, Wang J T, et al. Research on water immersion nonlinear ultrasonic mixing method for fatigue crack detection [J]. Journal of Vibration and Shock, 2023, 42(14): 204-210+244.
[13] Yan B S, Huang Z Y, Zhang B. Nonlinear Ultrasonic Testing and Signal Processing for Coating Quality of Magnesium Alloy [J]. Journal of Vibration, Measurement & Diagnosis, 2025, 45(06): 1098-1104+1270.
[14] Rucka M. Monitoring steel bolted joints during a monotonic tensile test using linear and nonlinear Lamb wave methods: A feasibility study[J]. Metals, 2018, 8(9): 683.
[15] Chai Y, Wu Q, Yan J J, et al. Failure monitoring and localization of wind turbine blades using ultrasonic guided waves and multi-index fusion imaging[J]. Engineering Failure Analysis, 2025,170: 109326.
[16] Zhou B, et al. An ultrasonic testing method for wall thickness of turbine blades[J]. Measurement, 2022,198: 111357.
[17] Sun H, Dong J, Diao X, et al. Crack detection method for wind turbine tower bolts using ultrasonic spiral phased array[J]. Sensors, 2024, 24(16): 5204.
[18] VDI 2230 Blatt 1. Systematische Berechnung hochbeanspruchter Schraubenverbindungen - Zylindrische Einschraubenverbindungen [S]. Düsseldorf: Verein Deutscher Ingenieure, 2003.
[19] He X L, Chen P, Liu H Q. Measurement method of bolt axial stress based on ultrasonic mode conversion [J]. Journal of Vibration and Shock, 2021, 40(21): 201-206.
[20] Abbate A, et al. Signal detection and noise suppression using a wavelet transform signal processor: application to ultrasonic flaw detection[J]. IEEE Transactions on Ultrasonics, Ferroelectrics, and Frequency Control, 2002, 44(1): 14-26.
[21] Song S P, Que P W. Wavelet based noise suppression technique and its application to ultrasonic flaw detection[J]. Ultrasonics, 2006, 44(2): 188-193.
[22] Sisojevs A, Tatarinov A, Kovalovs M, et al. An approach for parameters evaluation in layered structural materials based on DFT analysis of ultrasonic signals[C] // Proceedings of the International Conference on Pattern Recognition Applications and Methods (ICPRAM). Setubal, Portugal: SCITEPRESS, 2022: 307-314.
[23] Barth T, Rauter N. Determination of dispersion curves of higher order guided ultrasonic waves based on experimental data by a 2D-DFT[C] // Proceedings of the 10th European Workshop on Structural Health Monitoring (EWSHM 2024). Potsdam, Germany: e-Journal of Nondestructive Testing, 2024, 29(7).